

## Almost Circular Orbits in Classical Action-at-a-Distance Electrodynamics

C. M. Andersen and Hans C. von Baeyer

*Department of Physics, College of William and Mary, Williamsburg, Virginia 23185*

(Received 20 October 1971)

The motion of two fully relativistic classical spinless point particles interacting electromagnetically is studied in the special case of almost circular orbits. The equations of motion are *difference-differential* equations with half-retarded plus half-advanced Liénard-Wiechert potentials. As expected on both physical and mathematical grounds we find multiple stable solutions and conclude that ordinary (Newtonian) initial conditions are not sufficient to determine the trajectories. In addition to the stable solutions we find an infinity of divergent solutions. Alternatives for dealing with the extraneous solutions are discussed. The exact equations of motion can in certain limits be approximated by differential equations. Our solutions serve to delimit the range of applicability of the approximations.

### I. INTRODUCTION

Very little is known about the orbits of two classical relativistic point particles interacting electromagnetically. Even with the problems of self-energy and radiation circumvented by use of the time-symmetric Fokker action,<sup>1</sup> which contains particle coordinates but no field variables, the only known exact solutions are due to Schild<sup>2</sup> and have orbits which are concentric circles.<sup>3</sup> Several approximations to the theory have been studied. These provide useful checks on the solutions to the more general problem, but they shed no light on the questions of what happens when the particles come extremely close together (relative to the classical electron radius  $e^2/mc^2$ ), and of the uniqueness of the solutions given Newtonian initial conditions. Three such approximations are the following:

*i. The nonrelativistic approximation.* Darwin<sup>4</sup> has discussed the expansion in  $1/c$ , keeping terms of order  $1/c^2$ . He finds analytic solutions for any starting position and velocity. To order  $1/c^2$  the Lagrangian with fully retarded potentials (Darwin's case) and with one-half the retarded and one-half the advanced potentials (Fokker's case) are identical.<sup>5</sup> This surprising result is due to the fact that Darwin's correction terms are not, as he supposed, due to retardation but rather due to the magnetic interaction which exists even with no retardation.<sup>6</sup> Retardation effects, which will obviously be different for the two theories, are of higher order in  $1/c$ .

*ii. The potential-theory limit.* Synge<sup>7</sup> has considered the expansion in  $m_1/m_2$ . For  $m_2 = \infty$  he gives analytic solutions<sup>8</sup> for any starting position and velocity. The problem in this limit is that of a single particle moving relativistically in a fixed vector potential of the form  $A^\mu = (\gamma^{-1}, 0, 0, 0)$ . Since there is no recoil, the advanced and retarded po-

tentials coincide. For this reason there is again no distinction between the fully retarded theory and the Fokker theory.

*iii. The straight-line approximation.* Kerner<sup>9</sup> has considered the expansion in  $e^2$ . The retarded and advanced Liénard-Wiechert potentials are expanded about the equal-time point on the trajectory of the source particle. If only the opening term in  $e^2$  is retained, the theory is called the straight-line approximation<sup>10</sup> and consists of ordinary coupled differential equations. The name of this approximation stems from the observation that the potential would be exact if the source particle had constant velocity in the time interval between crossing the past and future light cones. Just as in the case of Darwin's approximation, the results to order  $e^2$  are identical for the fully retarded theory and the Fokker theory.

These approximations have not been worked out beyond their lowest terms, and the convergence properties of the expansions are not known.

In this paper we retain the time-symmetric Fokker action and find linear perturbations to Schild's circular orbits. Apart from keeping only first-order terms in the perturbation amplitude, our calculations are exact. In particular, they are valid for velocities in the entire range from zero to the velocity of light, for any ratio of rest masses of the two particles, and for any magnitude of the coupling constants. The results shed light on the questions of existence and uniqueness of solutions, stability of orbits, number of degrees of freedom, and selection principles for ruling out unphysical solutions.

The equations of motion resulting from the Fokker action principle do not form a system of simultaneous differential equations as in Newtonian mechanics. Instead they form a system of difference-differential equations because the three-ac-

celeration experienced by one particle depends on its own present position and velocity and on the past and future positions, velocities, and accelerations of the other particles. In general such equations are very difficult to solve. Even if solutions can be found the question remains whether Newtonian initial conditions, i.e., the positions and velocities of the two particles at some spacelike instants of time, are sufficient to specify a solution uniquely. Driver<sup>11</sup> has considered a number of problems of this type and has speculated that for most systems described by action-at-a-distance equations of motion the solution is *not* uniquely specified by Newtonian initial conditions.

The existence of multiple solutions has been expected on physical grounds. Plass,<sup>12</sup> who noticed multiple stable solutions for the motion of coupled one-dimensional oscillators, regarded the solutions as giving rise to new degrees of freedom, which he called "corporate" degrees of freedom. They do not arise when the oscillators are far apart, but as the oscillators are brought closer and closer together, more and more of them appear. Through their use Plass was able to derive the Rayleigh-Jeans law<sup>13</sup> for black-body radiation. According to him these corporate degrees of freedom take the place of the degrees of freedom of the electromagnetic field in conventional theory.

The particular system of equations to be solved for our problem of almost circular orbits is very complicated in its dependence on the parameters of the unperturbed orbit, but relatively simple in basic structure. We have a set of four coupled difference-differential equations which are linear and homogeneous in four unknown functions of time. These are the radial and azimuthal amplitudes for each particle. The arguments of these functions are  $t$ ,  $t + \tau$ , and  $t - \tau$ , where  $t$  is the (present) time and  $\tau$  is constant in time. It is because of the constancy of  $\tau$  that the equations are tractable.

Such a system of equations is known to reduce to an eigenvalue problem.<sup>14</sup> The eigenvalues depend on the velocities and are interpreted as complex frequencies of the normal modes. Our results, which are partly analytic and partly numerical, show the following pattern: At low velocities there are some real eigenvalues which correspond to trivial motions and one which corresponds to the almost elliptic orbits described by Darwin's solution, i.e., to a stable mode with the correct non-relativistic limit. In addition there is an infinity of complex eigenvalues, which correspond to divergent modes. (Some of these have been reported previously.<sup>15,16</sup>) The complex eigenvalues have imaginary parts which tend to infinity as the relative velocity approaches zero, i.e., they do not have a nonrelativistic limit. As the velocity in-

creases, the imaginary parts decrease and (for the equal-mass case) one of them reaches zero at a velocity of about  $0.95c$ . The corresponding real eigenvalue belongs to a new stable mode. As the velocity increases further, more eigenvalues reach the real axis and hence more stable solutions appear. In order to specify the solution of the equations at very high velocities it is therefore necessary to specify more than the 12 Newtonian initial conditions. The additional stable solutions are closely akin to Plass's corporate degrees of freedom. However, their continuation to divergent solutions at nonrelativistic velocities suggests that one should formulate a selection principle to rule them out.

Such selection principles are common in electrodynamics. We mention a few.

(i) In conventional classical electrodynamics Rohrlich's asymptotic condition,<sup>17</sup> patterned after the asymptotic condition in quantum field theory, decrees that as  $t \rightarrow \pm\infty$ , the acceleration should vanish. Clearly this principle is applicable to scattering problems but not to bound states.

(ii) The straight-line approximation to the Fokker theory selects those solutions which become straight lines as  $e^2 \rightarrow 0$ . This observation has been used by Kerner<sup>9</sup> to formulate a selection principle which admits only those solutions to the full theory which have the same property.

(iii) Van Dam and Wigner<sup>18</sup> have implicitly assumed a similar selection principle when they propose to find scattering solutions by successive approximation. The physically acceptable solutions are those which grow out of straight lines by iteration.

(iv) Synge<sup>7</sup> has described a method of solving the full equations by successive approximation starting with solutions for  $m_1/m_2 = 0$ . The solutions thus selected have potential-theory limits.

(v) Darwin's theory selects those solutions to the full theory which become solutions of the non-relativistic theory as  $c \rightarrow \infty$ . This observation can be used to formulate a correspondence principle: Physical solutions must have a nonrelativistic limit. Such a principle was used by Staruszkiewicz<sup>16</sup> to rule out unstable solutions.

(vi) Wheeler<sup>19</sup> suggested that divergent solutions be ruled out for physical reasons.

It may be that when more mathematical details are known, some of these selection principles will be identical.<sup>9</sup>

In our example one can adopt one of two points of view. If one accepts the correspondence principle (v), the solutions can be uniquely specified by Newtonian initial conditions and no corporate degrees of freedom appear. If one accepts Wheeler's stability condition (vi), then the solutions are not

unique and corporate degrees of freedom appear at very high velocities. The divergent solutions may be due to the perturbative treatment and perhaps do not survive in a fuller mathematical treatment. But even in this case we still have the problem of how to interpret the stable solutions. It may be of course that the whole problem does not arise in a more realistic theory which includes radiation or quantum effects or both.

## II. CIRCULAR ORBITS

Our starting point is Fokker's action integral for two point particles, labeled  $p$  and  $e$ , which have masses  $m_p$  and  $m_e$ , coordinates  $z_p^\mu$  and  $z_e^\mu$ , and charges  $e_p$  and  $e_e$ . Since we are concerned with an attractive vector interaction,  $e^2 \equiv -e_p e_e$  is a positive number. The action is

$$A = -m_p \int (\dot{z}_p^\mu \dot{z}_{p\mu})^{1/2} d\lambda_p - m_e \int (\dot{z}_e^\mu \dot{z}_{e\mu})^{1/2} d\lambda_e - e_p e_e \int \int \delta((z_p - z_e)^2) \dot{z}_p^\mu \dot{z}_{e\mu} d\lambda_p d\lambda_e, \quad (2.1)$$

where  $\lambda_p$  and  $\lambda_e$  parametrize the world lines and can be set equal to the proper times after the vari-

ational procedure, and where the dots refer to differentiation with respect to the appropriate  $\lambda$ . This action results in interactions only along light cones, and is symmetric under time reversal. The equations of motion are derived by requiring  $A$  to be stationary under variation of the world lines as functions of  $\lambda_p$  and  $\lambda_e$ . The resulting three-vector acceleration for particle  $e$  is

$$\tilde{\mathbf{a}}_e(t_e) = \frac{e_e}{m_e} (1 - v_e^2)^{1/2} \times \left( \tilde{\mathbf{E}} - \frac{\tilde{\mathbf{r}} \cdot \tilde{\mathbf{v}}_e \tilde{\mathbf{E}}}{r^0} + \frac{\tilde{\mathbf{r}} \tilde{\mathbf{v}}_e \cdot \tilde{\mathbf{E}}}{r^0} - \tilde{\mathbf{v}}_e \tilde{\mathbf{v}}_e \cdot \tilde{\mathbf{E}} \right)_{\text{ret, adv}}, \quad (2.2)$$

where  $\tilde{\mathbf{r}} = \tilde{\mathbf{r}}_p - \tilde{\mathbf{r}}_e$  and  $r_0 = t_p - t_e = \pm |\tilde{\mathbf{r}}|$ , depending on whether particle  $p$  is at its retarded or advanced position. The velocity  $\tilde{\mathbf{v}}_e$  is ordinary three-velocity. The right-hand side of Eq. (2.2) must be evaluated for the retarded and advanced positions of  $p$  and the results added and divided by two. In the large round parentheses the term independent of  $\tilde{\mathbf{v}}_e$  is electric in origin, the terms linear in  $\tilde{\mathbf{v}}_e$  are magnetic in origin, and the quadratic term is a relativistic correction. The electric field due to particle  $p$  and felt by  $e$  is given by

$$\tilde{\mathbf{E}}_{\text{ret, adv}} = \frac{\pm e_p}{(r^0 - \tilde{\mathbf{r}} \cdot \tilde{\mathbf{v}}_p)^3} \left[ (1 - v_p^2 + \tilde{\mathbf{r}} \cdot \tilde{\mathbf{a}}_p) (\tilde{\mathbf{r}} - r^0 \tilde{\mathbf{v}}_p) - r^0 \tilde{\mathbf{a}}_p (r^0 - \tilde{\mathbf{r}} \cdot \tilde{\mathbf{v}}_p) \right]_{\text{ret, adv}}. \quad (2.3)$$

The acceleration of particle  $p$  is obtained by interchanging the subscripts  $p$  and  $e$  in Eqs. (2.2) and (2.3). Together these four equations determine the dynamics.

Schild found that the circular-orbit solutions must satisfy

$$\frac{m_e}{e^2 \omega_0} = \frac{(1 - v_e^2)^{1/2}}{v_e (\theta_0 + v_e v_p \sin \theta_0)^3} [v_e + v_p (\cos \theta_0 - \theta_0^2 \cos \theta_0 + \theta_0 \sin \theta_0) + v_e^2 v_p (2 \cos \theta_0 + \theta_0 \sin \theta_0) + v_e v_p^2 (1 + \cos^2 \theta_0) + v_e^2 v_p^2 (v_e + v_p \cos \theta_0)] \quad (2.4)$$

and a similar expression with  $p$  and  $e$  interchanged. Here  $r_p = v_p/\omega_0$  and  $r_e = v_e/\omega_0$  are the radii of the orbits, and

$$\theta_0 = (v_e^2 + v_p^2 + 2v_e v_p \cos \theta_0)^{1/2} \quad (2.5)$$

is the retardation angle. This latter quantity, which is the same for both particles, is the angle through which one particle moves in the time it takes a light signal from the other particle to reach it. The retardation angle  $\theta_0$  ranges from zero to approximately 1.4782 (except in the potential limit, in which case  $\theta_0 = v_e$  and it ranges from zero to unity).

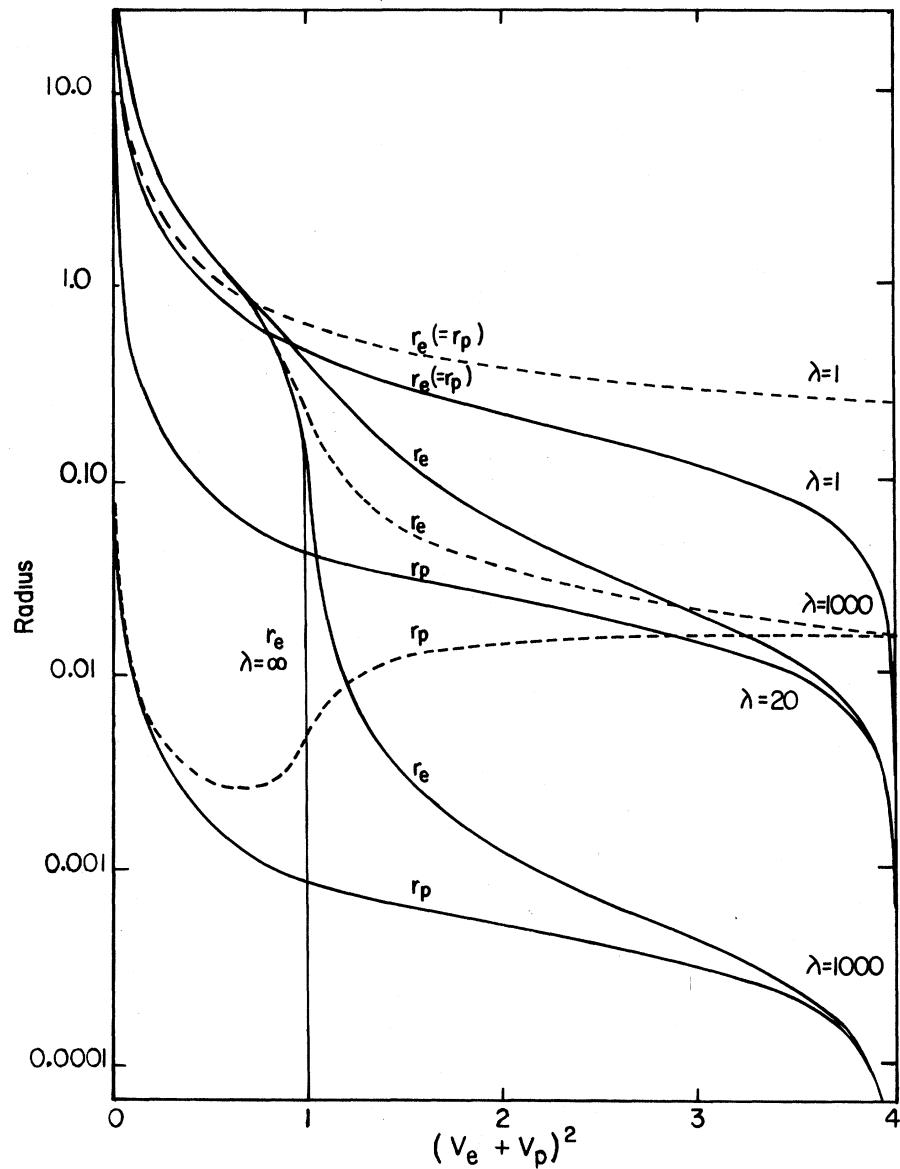
The solid curves of Fig. 1 show the variation of  $r_e$  and  $r_p$  with the square of the relative velocity,  $(v_e + v_p)^2$ , for  $m_p/m_e = 1, 20, 1000$ , and infinity. Note that as  $(v_e + v_p)^2$  goes to four,  $r_e/r_p$  approaches unity and  $r_e$  and  $r_p$  each approach zero.

In the potential-theory limit  $r_e$  approaches zero as  $(v_e + v_p)^2$  goes to unity. Here, as in the remainder of this paper, we have chosen the unit of length such that  $d \equiv m_r c^2/e^2 = 1$ , where  $m_r = m_p m_e/(m_p + m_e)$  is the reduced rest mass,  $c = 1$ , and  $e^2 = -e_p e_e$ . We specify  $\theta_0$  and  $v_p$ , determine  $v_e$  from Eq. (2.5), and then determine  $m_p/m_e$  from the ratio of Eq. (2.4) to its analog for  $m_p$ . By relating this ratio to the quantity  $d = 1$  we solve for  $m_p/e^2$  and  $m_e/e^2$ , then for  $\omega_0$ , and finally for  $r_p = v_p/\omega_0$  and  $r_e = v_e/\omega_0$ .

At this point we have found the solutions for circular orbits. Energy and angular momentum can then be found from formulas given by Schild.<sup>2</sup> Representative curves of angular momentum vs energy for circular orbits can be found in a previous work.<sup>3</sup>

In comparison with Eq. (2.4) the three limits or approximations discussed above yield the following:

FIG. 1. Radii of the two particles in concentric circular orbits vs the relative velocity squared. The solid curves show the exact solutions when the mass ratio  $\lambda = m_p/m_e$  takes on the values 1, 20, 1000, and infinity. The dashed curves show the results of using the straight-line approximation for  $\lambda = 1$  and 1000. For  $\lambda = \infty$  the straight-line approximation is exact.



(i) The nonrelativistic approximation.

$$\frac{m_e}{e^2 \omega_0} = \frac{1}{v_e(v_e + v_p)^2} \left[ 1 - \frac{1}{2}(v_e^2 + v_p^2) \right],$$

$$\frac{m_p}{e^2 \omega_0} = \frac{1}{v_p(v_e + v_p)^2} \left[ 1 - \frac{1}{2}(v_e^2 + v_p^2) \right].$$

(ii) The potential-theory limit.

$$\frac{m_e}{e^2 \omega} = \frac{(1 - v_e^2)^{1/2}}{v_e^3},$$

$$v_p = 0.$$

(iii) The straight-line approximation.

$$\frac{m_e}{e^2 \omega_0} = \left( \frac{1 - v_e^2}{1 - v_p^2} \right)^{1/2} \frac{1 + v_e v_p}{v_e(v_e + v_p)^2},$$

$$\frac{m_p}{e^2 \omega_0} = \left( \frac{1 - v_p^2}{1 - v_e^2} \right)^{1/2} \frac{1 + v_e v_p}{v_p(v_e + v_p)^2}.$$

(2.8)

The dashed curves of Fig. 1 show the variation of  $r_e$  and  $r_p$  with  $v_r^2 = (v_e + v_p)^2$  in the straight-line approximation. This approximation has the same nonrelativistic and potential-theory limits as the exact theory. In addition, the ratio  $r_e/r_p$  approaches unity as  $v_r^2$  goes to four, just as in the exact theory. However, in this approximation the two radii approach a finite limit  $\frac{1}{2}(m_e m_p)^{1/2}/(m_e + m_p)$ , whereas they approach zero in the exact theory.

Also we note that, unlike in Darwin's nonrelativistic approximation, the first correction terms in  $v^2$  are wrong.<sup>20</sup> We conclude that the straight-line approximation is not adequate for the description of relativistic circular orbits.

### III. THE EQUATIONS FOR ALMOST CIRCULAR MOTION

We work in the center-of-mass frame, let  $t_p = t_e = t$ , and write the time dependence of the polar coordinates of the particles as

$$\begin{aligned} r_e(t) &= r_e[1 + \lambda \rho_e(t)], \\ \phi_e(t) &= \pi + \omega_0 t + \lambda \epsilon_e(t), \\ r_p(t) &= r_p[1 + \lambda \rho_p(t)], \\ \phi_p(t) &= \omega_0 t + \lambda \rho_p(t), \end{aligned} \quad (3.1)$$

where  $r_e$  and  $r_p$  (without arguments) are the unperturbed radii and  $\omega_0$  is the unperturbed angular velocity. The parameter  $\lambda$  symbolizes the infinites-

imal character of the perturbations. Terms in  $\lambda^2$  are dropped. The four functions  $\rho_e(t)$ ,  $\rho_p(t)$ ,  $\epsilon_e(t)$ , and  $\epsilon_p(t)$  are to be determined by solving Eqs. (2.2) and (2.3) and the corresponding equations for  $\vec{a}_p$ . The advanced and retarded points on the  $p$  trajectory which appear in Eqs. (2.2) and (2.3) are lightlike with respect to the point at time  $t$  on the world line of  $e$ . In the case of circular orbits, the time advance and time delay are constant in time and equal in magnitude to  $\theta_0/\omega_0$ . For almost circular orbits they deviate only in first order in  $\lambda$  from  $\theta_0/\omega_0$ . This observation is very important because it allows us to express the equations for almost circular motion in terms of the positions, velocities, and accelerations at the same equally spaced points in time ( $t + \theta_0/\omega_0$ ,  $t$ ,  $t - \theta_0/\omega_0$ ) as in the unperturbed case.

Let  $\theta_{e,r} = \omega_0(t - t_r)$  and  $\theta_{e,a} = \omega_0(t - t_a)$ , where  $t$  is the present time and  $t_r$  and  $t_a$  are the retarded and advanced times, respectively, when  $p$  is lightlike [ $(z_p - z_e)^2 = 0$ ] to  $e$ . Let  $k$  stand for either  $r$  or  $a$  and we have

$$(t - t_k)^2 = |\vec{z}_e(t) - \vec{z}_p(t_k)|^2 \cong r_e^2[1 + 2\lambda\rho_e(t)] + r_p^2[1 + 2\lambda\rho_p(t)] + 2r_e r_p[1 + \lambda\rho_e(t) + \lambda\rho_p(t_k)] \cos\{\omega_0(t - t_k) + \lambda[\epsilon_e(t) - \epsilon_p(t_k)]\}. \quad (3.2)$$

Then

$$\theta_{e,k} = \theta_{0,k} + \lambda(v_e^2\rho_e(t) + v_p^2\rho_p(t_k) + v_e v_p[\rho_e(t) + \rho_p(t_k)] \cos\theta_{0,k} - [\epsilon_e(t) - \epsilon_p(t_k)] \sin\theta_{0,k}) / (\theta_{0,k} + v_e v_p \sin\theta_{0,k}), \quad (3.3)$$

where  $\theta_{0,r} = \theta_0$  and  $\theta_{0,a} = -\theta_0$  and where  $v_e$  and  $v_p$  are the unperturbed velocities. Let  $\theta_{p,r}$  and  $\theta_{p,a}$  be similarly defined. Then an expression for  $\theta_{p,k}$  analogous to Eq. (3.3) holds.

The next step is to express the quantities appearing in Eqs. (2.2) and (2.3) and their counterparts for  $\vec{a}_p$  in terms of the  $\rho$ 's and the  $\epsilon$ 's of Eq. (3.1). For example, we have

$$\begin{aligned} x_e(t) &= -r_e \left\{ [1 + \lambda\rho_e(t)] \cos\omega_0 t - \lambda\epsilon_e(t) \sin\omega_0 t \right\}, \\ y_e(t) &= -r_e \left\{ [1 + \lambda\rho_e(t)] \sin\omega_0 t + \lambda\epsilon_e(t) \cos\omega_0 t \right\}, \end{aligned} \quad (3.4)$$

and

$$\begin{aligned} x_p(t_k) &= x_p \left( t - \frac{\theta_{0,k}}{\omega_0} - \frac{\theta_{e,k} - \theta_{0,k}}{\omega_0} \right) \\ &= x_p \left( t - \frac{\theta_{0,k}}{\omega_0} \right) - (\theta_{e,k} - \theta_{0,k}) \omega_0^{-1} v_{xp} \left( t - \frac{\theta_{0,k}}{\omega_0} \right) \\ &= r_p \left\{ \left[ 1 + \lambda\rho_p \left( t - \frac{\theta_{0,k}}{\omega_0} \right) \right] \cos(\omega_0 t - \theta_{0,k}) \right. \\ &\quad \left. - \left[ \lambda\epsilon_p \left( t - \frac{\theta_{0,k}}{\omega_0} \right) - (\theta_{e,k} - \theta_{0,k}) \right] \sin(\omega_0 t - \theta_{0,k}) \right\}, \end{aligned} \quad (3.5a)$$

$$\begin{aligned} y_p(t_k) &= r_p \left\{ \left[ 1 + \lambda\rho_p \left( t - \frac{\theta_{0,k}}{\omega_0} \right) \right] \sin(\omega_0 t - \theta_{0,k}) \right. \\ &\quad \left. + \left[ \lambda\epsilon_p \left( t - \frac{\theta_{0,k}}{\omega_0} \right) - (\theta_{e,k} - \theta_{0,k}) \right] \cos(\omega_0 t - \theta_{0,k}) \right\}. \end{aligned} \quad (3.5b)$$

Similar expressions are used for the components of  $\vec{z}_p(t)$ ,  $\vec{z}_e(t_k)$ , and for the relevant velocities and accelerations. The result is a set of four coupled second-order difference-differential equations which are linear and homogeneous in the  $\rho$ 's and  $\epsilon$ 's.

Because the problem is time-symmetric, we can find solutions of the form

$$\begin{aligned} \rho_e(t) &= F_e \sin\omega t, \\ \epsilon_e(t) &= G_e \cos\omega t, \\ \rho_p(t) &= F_p \sin\omega t, \\ \epsilon_p(t) &= G_p \cos\omega t. \end{aligned} \quad (3.6)$$

This parametrization leads us to the eigenvalue equation

$$\begin{pmatrix} A_{e02}\omega^2 - A_{e00} & A_{e01}\omega & A_{p+2}\omega^2 \cos \xi & A_{p-2}\omega^2 \sin \xi \\ & & -A_{p-1}\omega \sin \xi & +A_{p+1}\omega \cos \xi \\ & & -A_{p+0} \cos \xi & -A_{p-0} \sin \xi \\ B_{e01}\omega & -B_{e02}\omega^2 + B_{e00} & B_{p-2}\omega^2 \sin \xi & -B_{p+2}\omega^2 \cos \xi \\ & & +B_{p+1}\omega \cos \xi & +B_{p-1}\omega \sin \xi \\ & & -B_{p-0} \sin \xi & +B_{p+0} \cos \xi \\ A_{e+2}\omega^2 \cos \xi & A_{e-2}\omega^2 \sin \xi & A_{p02}\omega^2 - A_{p00} & A_{p01}\omega \\ -A_{e-1}\omega \sin \xi & +A_{e+1}\omega \cos \xi & & \\ -A_{e+0} \cos \xi & -A_{e-0} \sin \xi & & \\ B_{e-2}\omega^2 \sin \xi & -B_{e+2}\omega^2 \cos \xi & B_{p01}\omega & -B_{p02}\omega^2 + B_{p00} \\ +B_{e+1}\omega \cos \xi & +B_{e-1}\omega \sin \xi & & \\ -B_{e-0} \sin \xi & +B_{e+0} \cos \xi & & \end{pmatrix} \begin{pmatrix} F_e \\ G_e \\ F_p \\ G_p \end{pmatrix} = 0, \quad (3.7)$$

where  $\xi = \theta_0 \omega / \omega_0$ . The dependence of the  $A$ 's and  $B$ 's on the parameters  $v_e$ ,  $v_p$ ,  $\theta_0$ , and  $\omega_0$  of the unperturbed orbits is given in the Appendix. The  $A$ 's are determined from the radial equations of motion while the  $B$ 's come from the tangential equations of motion. Since great care is required in deriving these expressions, we have written a FORMAC language computer program to do much of the lengthy and tedious algebra.

Let the square matrix in Eq. (3.7) hereafter be called  $M$ . Then Eq. (3.7) has solutions for those values of  $\omega$  for which the determinant  $D$  of  $M$  is zero. The stable perturbed orbits (those with real  $\omega$ ) are rotating ellipses whose perihelion advances at the rate of  $2\pi(\omega_0 - |\omega|)/|\omega|$  radians per revolution. The form of Eq. (3.7) is such that if  $\omega$  is an eigenvalue, then  $-\omega$ ,  $\bar{\omega}$ , and  $-\bar{\omega}$  are also eigenvalues. ( $\bar{\omega}$  is the complex conjugate of  $\omega$ .) However,  $\omega$  and  $-\omega$  always lead to the same solutions. Further, if  $\omega$  is a complex number, then there is only one real solution associated with these four eigenvalues.

In the case  $m_e = m_p$ , we have  $v_e = v_p$  and Eq. (3.7) can be simplified.  $M$  now has the form

$$\begin{pmatrix} \omega^2 + \omega_0^2[3 + v_e^2/(1 - v_e^2)] & -\omega\omega_0[2 + v_e^2/(1 - v_e^2)] & 0 & 0 \\ \omega\omega_0(2 - v_e^2) & -\omega^2 & 0 & 0 \\ \dots & \dots & \omega^2 + \omega_0^2 & -2\omega\omega_0 \\ \dots & \dots & 2\omega\omega_0 & -(\omega^2 + \omega_0^2) \end{pmatrix} \begin{pmatrix} F_e \\ G_e \\ F_p \\ G_p \end{pmatrix} = 0, \quad (3.10)$$

where the entries in the lower left submatrix are complicated and of no consequence. Two of the eigenvalues of Eq. (3.10) are  $\omega = \pm\omega_0(1 - v_e^2)^{1/2}$ . Both of these eigenvalues correspond to the potential-theory solution,<sup>3</sup> a precessing ellipse whose perihelion advances for low velocities at the rate of  $2\pi(\omega_0 - |\omega|)/|\omega| \cong \pi v_e^2$  radians per revolution. In addition, the determinant of the matrix in Eq.

$$M = \begin{pmatrix} A & B & C & D \\ E & F & G & H \\ C & D & A & B \\ G & H & E & F \end{pmatrix}, \quad (3.8)$$

and the block-diagonal matrix

$$M' = \begin{pmatrix} A+C & B+D & 0 & 0 \\ E+G & F+H & 0 & 0 \\ 0 & 0 & A-C & B-D \\ 0 & 0 & E-C & F-H \end{pmatrix} = \begin{pmatrix} M^{(+)} & 0 \\ 0 & M^{(-)} \end{pmatrix} \quad (3.9)$$

can easily be shown to have the same determinant as  $M$ . Thus a zero of  $D$  is associated either with a zero of  $D^{(+)} = \det(M^{(+)})$  or of  $D^{(-)} = \det(M^{(-)})$ . Zeros of  $D^{(+)}$  correspond to eigenvalues with  $F_e = F_p$  and  $G_e = G_p$ , while zeros of  $D^{(-)}$  correspond to eigenvalues with  $F_e = -F_p$  and  $G_e = -G_p$ . In this manner the problem has been reduced from a four-dimensional one to a two-dimensional one.

In the case  $m_p \rightarrow \infty$ , Eq. (3.7) becomes

(3.10) has double roots at  $0, \pm\omega_0$ . These correspond to trivial solutions. The eigenvalue  $\omega = 0$  has  $(F_e, G_e, F_p, G_p) = (0, 1, 0, 1)$ , which corresponds to a circular orbit with the azimuthal angle differing by a constant amount from the unperturbed orbit. It is easy to check that  $\omega = 0$  with eigenvector  $(0, 1, 0, 1)$  is also a trivial solution for the general equation (3.7). The values  $\omega = \pm\omega_0$  of Eq. (3.10) correspond

to the eigenvector  $(0, 0, 1, 1)$ . Since  $v_p = 0$  we see from Eqs. (3.1) and (3.6) that this seems to correspond to no perturbation at all. However, the general equation (3.7) also has trivial solutions of this type. The eigenvalues are  $\omega = \pm\omega_0$  and the eigenvectors are  $(v_p, v_p, \mp v_e, \mp v_e)$ . The interpretation here is that the corresponding solutions have again just circular orbits. The  $p$  and  $e$  orbits are concentric but their common center is slightly displaced from the origin. In the  $v_p = 0$  limit we still have physical solutions of this type.

#### IV. ASYMPTOTIC EXPRESSIONS FOR THE EIGENVALUES $\omega$

The determinant  $D$  of the matrix  $M$  can be written in the form

$$D = e^{-4s} \sum_{k=0}^8 \sum_{j=0}^8 a_{jk} s^j e^{ks}, \quad (4.1)$$

where  $s = i\xi = i\theta_0(\omega/\omega_0)$  and the  $a_{jk}$  are real functions of the parameters of the unperturbed orbit. Such a form is usually called an *exponential polynomial* or a *quasipolynomial*. Without numerical computation, little can be accomplished toward finding the zeros of  $D$  with small magnitude of  $s$ . However, for those zeros with large imaginary part of  $s$  there are useful asymptotic formulas.<sup>21</sup>

For simplicity consider the case  $m_e = m_p$  and  $v_e = v_p \equiv v < 1$ . The determinants  $D^{(\pm)}$  have the form

$$D^{(\pm)} = e^{-2s} \sum_{k=0}^4 \sum_{j=0}^4 a_{jk}^{(\pm)} s^j e^{ks}, \quad (4.2)$$

where the  $a_{jk}^{(+)}$  correspond to the two-dimensional matrix  $M^{(+)}$  and the  $a_{jk}^{(-)}$  correspond to  $M^{(-)}$ . Further, because  $A_{+2}B_{+2} = A_{-2}B_{-2}$  (we have dropped the first subscript on the  $A$ 's and  $B$ 's because it is superfluous in the equal-mass case), we have  $a_{0,4}^{(+)} = a_{4,4}^{(+)} = 0$ . In Fig. 2 we construct a diagram in which we place a dot with abscissa  $k$  and ordinate  $j$  for each pair of integers  $(k, j)$  with  $a_{jk} \neq 0$ . We then construct a polygonal line which must (i) have vertices only at these dots, (ii) be convex upward (or straight), (iii) have no dots above it, and (iv) extend from the leftmost column of the dots to the rightmost column. This graph ( $L_1, L_2, L_3$ ) is known as the distribution diagram for the exponential polynomial (4.2). The terms which correspond to the dots beneath this graph may have a strong effect on the location of the zeros with small  $|s|$ . However, they may be ignored for purposes of finding the asymptotic formulas. The five terms of Eq. (4.2) which correspond to the five dots through which the graph passes are the only ones which contribute asymptotically. Thus

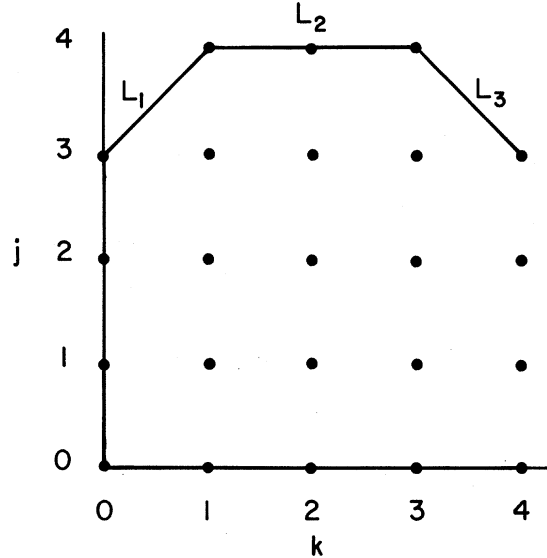


FIG. 2. Distribution diagram for the exponential polynomials  $D^{(\pm)}$  ( $s$ ). The integer  $k$  is the coefficient of  $s$  in the exponential and  $j$  is the power of  $s$ . The dots refer to the terms  $a_{jk} s^j e^{ks}$  with  $a_{jk} \neq 0$  in  $D^{(\pm)}$  ( $s$ ). The three straight-line segments  $L_1, L_2$ , and  $L_3$  comprise the distribution diagram. The points and the distribution diagram for  $D^{(-)}$  ( $s$ ) are identical with those for  $D^{(+)}$  ( $s$ ).

$$e^{2s} D^{(\pm)} \cong a_{3,0}^{(\pm)} s^3 + a_{4,1}^{(\pm)} s^4 e^s + a_{4,2}^{(\pm)} s^4 e^{2s} + a_{4,3}^{(\pm)} s^4 e^{3s} + a_{3,4}^{(\pm)} s^3 e^{4s}, \quad (4.3)$$

with

$$a_{3,0}^{(\pm)} = -a_{3,4}^{(\pm)} = \frac{1}{4}(\omega_0/\theta_0)^3 (A_{+2}B_{-1} + A_{-1}B_{+2} - A_{+1}B_{-2} - A_{-2}B_{+1}) - \frac{1}{2}\omega_0^4,$$

$$a_{4,1}^{(\pm)} = a_{4,3}^{(\pm)} = \pm \frac{1}{2}(\omega_0/\theta_0)^4 (A_{02}B_{+2} + A_{+2}B_{02}) \pm \omega_0^4 / (16v^2), \quad (4.4)$$

$$a_{4,2}^{(\pm)} = (\omega_0/\theta_0)^4 (A_{02}B_{02} + A_{+2}B_{+2}) - \omega_0^4 / (16v^4).$$

The arrows show nonrelativistic limits.

The zeros of  $D^{(\pm)}$  asymptotically fall into four sets of chains, one chain associated with the straight-line segment  $L_1$  (cf. Fig. 2), two with  $L_2$ , and one with  $L_3$ . The zeros associated with  $L_3$  are determined only by the coefficients  $a_{3,4}^{(\pm)}$  and  $a_{4,3}^{(\pm)}$ . Dropping over-all factors we are led to the equation

$$s \pm (2v^2)e^s = 0. \quad (4.5)$$

The asymptotic formula for its zeros is

$$\begin{aligned} \text{Res} &= -\ln(2v^2) + \ln| \text{Im}s |, \\ \text{Im}s &= (2k \mp \frac{1}{2}k / |k|) \pi, \end{aligned} \quad (4.6)$$

where upper (lower) signs refer to  $D^{(+)}$  ( $D^{(-)}$ ) and  $k$  is any large positive or negative integer. Similarly, line segment  $L_1$  corresponds to

$$2v^2 \mp se^s = 0 \quad (4.7)$$

with the asymptotic formula

$$\begin{aligned} \text{Res} &= \ln(2v^2) - \ln|\text{Im}s|, \\ \text{Im}s &= (2k \mp \frac{1}{2}k/|k|)\pi. \end{aligned} \quad (4.8)$$

Finally, associated with line segment  $L_2$  we have the three terms with  $(k, j)$  values of  $(1, 4)$ ,  $(2, 4)$ , and  $(3, 4)$ . When we drop over-all factors we are left with

$$1 \pm 2v^2 \text{cosh}s = 0, \quad (4.9)$$

which has the approximate solutions

$$s = 2 \ln v + (2k + \frac{1}{2} \pm \frac{1}{2})\pi i \quad (4.10)$$

and

$$s = -2 \ln v + (2k + \frac{1}{2} \pm \frac{1}{2})\pi i, \quad (4.11)$$

where again upper (lower) signs correspond to  $D^{(+)}$  ( $D^{(-)}$ ) and  $k$  is any positive or negative integer. Staruszkiewicz<sup>22</sup> discovered the solutions (4.10) and (4.11) associated with  $L_2$  but overlooked those associated with  $L_1$  and  $L_3$ .

The transition from the variable  $s$  to the variable  $\omega/\omega_0$  is simple and results in the following four chains of asymptotic zeros for  $D^{(\pm)}$  for  $v \ll 1$ :

$$\omega/\omega_0 = (k \mp \frac{1}{4}k/|k|)\pi/v + \frac{i}{2v} \ln |(k \mp \frac{1}{4}k/|k|)\pi/v^2|, \quad (4.12)$$

$$\omega/\omega_0 = (k + \frac{1}{4} \pm \frac{1}{4})\pi/v + \frac{i}{2v} \ln |1/v^2|, \quad (4.13)$$

$$\omega/\omega_0 = (k + \frac{1}{4} \pm \frac{1}{4})\pi/v - \frac{i}{2v} \ln |1/v^2|, \quad (4.14)$$

$$\omega/\omega_0 = (k \mp \frac{1}{4}k/|k|)\pi/v - \frac{i}{2v} \ln |(k \mp \frac{1}{4}k/|k|)\pi/v^2|. \quad (4.15)$$

In each chain the approximation to the true zeros of  $D^{(\pm)}$  becomes better and better as the integer  $k$  becomes larger in magnitude.

For the case  $m_e \neq m_p$  we must revert back to Eq. (4.1). Though we have not worked out many details, we can point out that  $a_{80} = a_{81} = a_{87} = a_{88} = 0$  and that Eq. (4.9) generalizes to

$$1 \pm (v_e v_p)^{1/2} (v_e + v_p) \text{cosh}s = 0. \quad (4.16)$$

If we let  $y^2 = m_p/m_e$ , then the asymptotic solutions of Eq. (4.16) are

$$\begin{aligned} \omega/\omega_0 &= (v_e + v_p)^{-1} (2k + \frac{1}{2} \pm \frac{1}{2})\pi \\ &\quad + i(v_e v_p)^{-1} \ln |4/(v_e + v_p)^2| \\ &\quad + i(v_e + v_p)^{-1} \ln |\frac{1}{2}(y + y^{-1})| \end{aligned} \quad (4.17)$$

and

$$\begin{aligned} \omega/\omega_0 &= (v_e + v_p)^{-1} (2k + \frac{1}{2} \pm \frac{1}{2})\pi \\ &\quad - i(v_e + v_p)^{-1} \ln |4/(v_e + v_p)^2| \\ &\quad - i(v_e + v_p)^{-1} \ln |\frac{1}{2}(y + y^{-1})|. \end{aligned} \quad (4.18)$$

In the equal-mass case  $y=1$  and Eqs. (4.17) and (4.18) are the same as Eqs. (4.13) and (4.14). In the unequal-mass case the last terms of Eqs. (4.17) and (4.18) move the zeros farther and farther without limit away from the real axis as  $y$  goes from unity to infinity. We expect a similar behavior for the zeros approximated by Eqs. (4.12) and (4.15), so that in the potential-theory limit we are left with no complex eigenvalues at all.

## V. NUMERICAL SOLUTIONS FOR THE EQUAL-MASS CASE

In this section we return to the equal-mass case. We resort to numerical computation in order to lift our previous restrictions to low velocities and to large real part of  $\omega/\omega_0$  (i.e., large imaginary part of  $s$ ). Figure 3 shows how a few of these zeros vary in the complex  $\omega$  plane as the velocity  $v$  varies. The solid (dashed) curves represent zeros of  $D^{(+)}$  ( $D^{(-)}$ ). For low velocities there are some zeros lying on the real axis between  $-1$  and  $+1$ . These we will discuss later. The remaining zeros are infinite in number, are complex, and are approximated by the four chains (4.12) to (4.15). In Fig. 3 we have marked the positions of these zeros for velocities of 0.10 and 0.314. In addition for  $v=0.1$ , we have plotted exact solutions of the asymptotic equations (4.7) and (4.9) and their approximations by the asymptotic formulas (4.13) and (4.12). We see that Eq. (4.7) is considerably more accurate for small  $k$  than Eq. (4.13), but that Eq. (4.13) has become quite good for  $k \geq 3$ .

There are four zeros (two each in the upper and lower half planes) which are pure imaginary at low velocities. At  $v \cong 0.12$  they collide in pairs and leave the imaginary axis. Then at  $v \cong 0.95$  they become the first complex zeros to move onto the real axis. They belong to solutions of  $D^{(-)}$ , i.e., solutions with  $F_p = -F_e$ ,  $G_p = -G_e$ . The other zeros in the  $L_1$  and  $L_3$  series also move onto the real axis as the velocity becomes higher and higher. The zeros in the  $L_2$  series move toward the origin at low velocities but at high velocities they swerve and move away from the real axis.

In addition to those zeros which are complex at low velocities, there are some which are real for all velocities. These are the fixed zeros at  $\omega/\omega_0 = 0, \pm 1$ , which we discussed in Sec. III, and the zeros of  $D^{(+)}$  which begin at  $\omega/\omega_0 = \pm 1$  for  $v=0$  and move toward the origin as  $v$  approaches unity. The solution which corresponds to this latter pair of zeros coincides to order  $v^2$  with Darwin's solution. The solid equal-mass curve of Fig. 4 shows the variation of  $\omega/\omega_0$  with  $v_r^2 = (v_e + v_p)^2$ . For low velocities we have

$$\omega/\omega_0 = 1 - 2v^2 = 1 - \frac{1}{2}v_r^2 \quad (5.1)$$



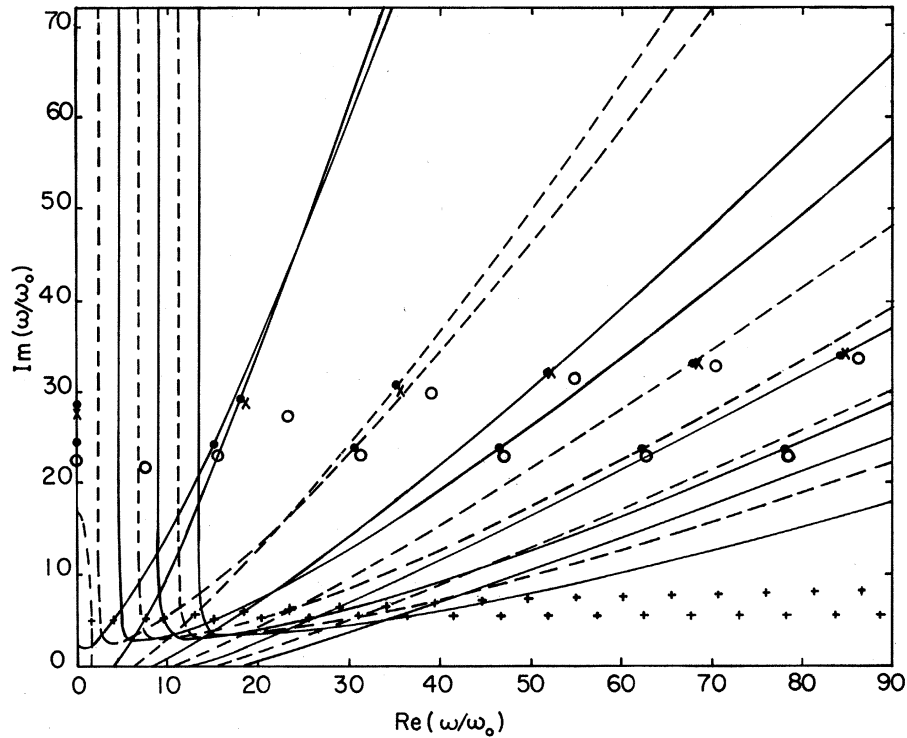


FIG. 3. Motion for  $m_p = m_e$  of a few of the zeros  $\omega/\omega_0$  in the complex plane as the velocity varies from zero to unity. The symbols  $\bullet$  and  $+$  show the positions of the zeros for  $v=0.10$  and  $v=0.314$ , respectively. The symbol  $x$  shows exact solutions of the asymptotic equations (4.7) for  $v=0.10$ . The symbol  $\circ$  shows solutions given by the asymptotic formulas (4.13) and (4.12) for  $v=0.10$ . The trajectories exhibit mirror symmetry about both the real and imaginary axes.

in agreement with Darwin. Along this curve the rate of the perihelion advance varies from zero (at  $v=0$ ) to infinity (at  $v=1$ ). For very high velocities this means that there are several revolutions between perihelia. The dashed (equal-mass) curve in Fig. 4 belongs to those stable solutions of  $D^{(-)}$  whose continuations to low velocities have imaginary  $\omega$ . Similar curves occur at higher values of  $\omega/\omega_0$  for both  $D^{(+)}$  and  $D^{(-)}$ . The corresponding solutions are stable and typically have many perihelia per revolution.

In general the eigenvectors can be specified up to normalization by giving, for example, the three ratios  $F_e/G_e$ ,  $F_p/F_e$ , and  $G_p/F_p$ . In the equal-mass case  $F_e/G_e = F_p/G_p$  and  $F_p/F_e = \pm 1$ .  $F_e/G_e$  has the following geometric interpretation. Let the perturbed orbit be viewed in the noninertial coordinate system whose center is located at  $(-r_e \cos \omega_0 t, -r_e \sin \omega_0 t)$  and whose  $x$  axis rotates so as to be radially outward from the old origin. Then a perfectly circular orbit with angular velocity  $\omega_0$  is seen as a fixed point at the origin of the new coordinate system. A perturbation of this circular orbit with the same average angular velocity [cf. Eq. (3.4)] will be seen in the new coordinate system as a closed ellipse of length  $2\lambda r_e F_e$  along the  $x$  axis

and  $2\lambda r_e G_e$  along the  $y$  axis. This ellipse is traversed in the time  $2\pi/\omega$ , and the ratio of its  $x$  axis to its  $y$  axis is  $F_e/G_e$ . The equal-mass curves of Fig. 5 show the variation of this ratio with  $v_r^2$ . For low velocities on the normal equal-mass curve ( $F_p = F_e$ ,  $G_p = G_e$ ), we get

$$F_e/G_e = \frac{1}{2}(1 - v^2) = \frac{1}{2}(1 - \frac{1}{4}v_r^2). \quad (5.2)$$

For very high velocities on this curve  $F_e/G_e$  tends to zero, meaning that the perturbation is mainly in the tangential direction. The higher-order stable solutions are characterized by high values of  $F_e/G_e$ . This means that for them the perturbation is mainly along the radial direction.

## VI. SOLUTIONS FOR THE CASE OF UNEQUAL MASS

As the mass ratio  $\lambda = m_p/m_e$  varies from unity to infinity, we should expect our equal-mass solutions to gradually deform into the solutions discussed by Sommerfeld for the potential-theory limit. But as we have observed before,<sup>3</sup> this is a tricky limit to take. For any very large but finite mass ratio  $\lambda$ , as  $v_e$  approaches unity the effective mass of  $e$  increases and becomes comparable to the rest mass

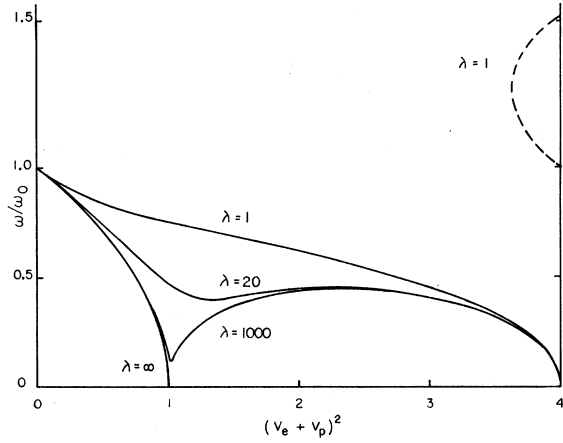


FIG. 4. The variation of  $\omega/\omega_0$  with relative velocity squared for different values of the mass ratio  $\lambda = m_p/m_e$ . The solid  $\lambda = 1$  curve has  $F_p = F_e$  and  $G_p = G_e$ , while the dashed  $\lambda = 1$  curve has  $F_p = -F_e$  and  $G_p = -G_e$ . Not shown are additional solutions for  $\lambda = 1$  with large relative velocities and large  $\omega/\omega_0$ .

of  $p$ , resulting in  $v_p$  approaching unity also. Thus the upper limit of  $v_r^2 = (v_e + v_p)^2$  is always four. However, in the strict potential-theory limit  $v_p$  is equal to zero and so the upper limit of  $v_r^2$  is unity rather than four (cf. Fig. 1). Similarly, the total energy for two particles in concentric circular orbits for any finite  $\lambda$  goes to zero as their velocities approach unity. However, in the potential-theory limit, by not treating the case where  $v_p$  is appreciably different from zero, one concludes that the total energy goes to  $m_p c^2$  which is infinite.

In Fig. 4 we show graphs of  $\omega/\omega_0$  vs  $v_r^2$  for the stable solutions for mass ratios  $\lambda = 1, 20, 1000$ ,

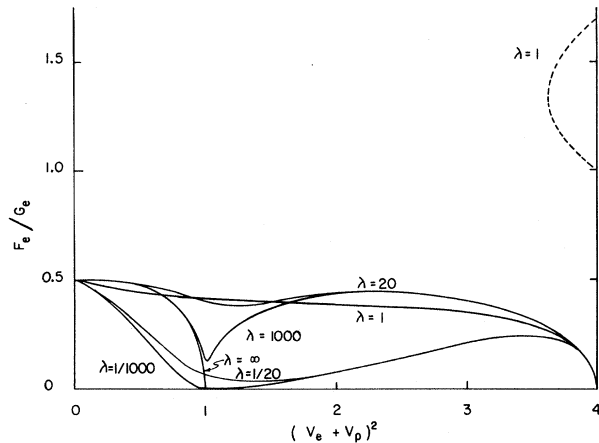


FIG. 5. The ratio of the radial perturbation to the tangential perturbation shown as a function of the relative velocity squared for different values of the mass ratio  $\lambda = m_p/m_e$ . The additional solutions for  $\lambda = 1$  have still higher values of  $F_e/G_e$ .

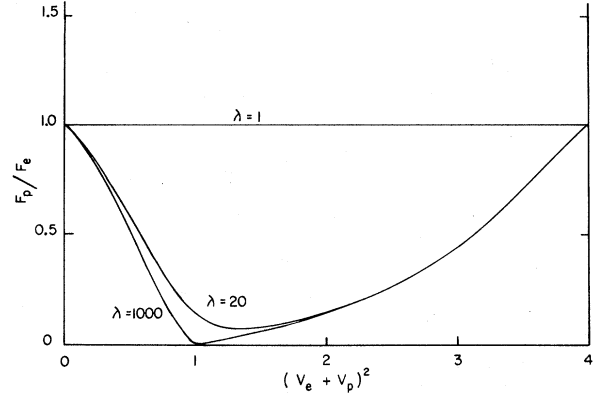


FIG. 6. The variation of  $F_p/F_e$  with relative velocity squared for three different values of the mass ratio  $\lambda = m_p/m_e$ . The heavier particle experiences a smaller percentage change in its radius as a function of time than the lighter particle does. The dashed  $\lambda = 1$  curves (not shown) have  $F_p/F_e = -1$ .

and  $\infty$ . For  $0 < v_r^2 < 1$  we see that as  $\lambda$  becomes large the  $\omega/\omega_0$  curves approach the potential-theory limit,  $\omega/\omega_0 = (1 - v_r^2)^{1/2}$ . But potential theory gives no clue as to the limiting values of  $\omega/\omega_0$  for  $1 < v_r^2 < 4$ .

Next we turn to the eigenvectors. In Fig. 5 we show graphs of  $F_e/G_e$  vs  $v_r^2$  for stable solutions for mass ratios  $\lambda = 1/1000, 1/20, 1, 20, 1000$ . The  $\lambda = 1/1000$  and  $1/20$  curves are included because the ratio  $F_p/G_p$  for  $\lambda = 1000$  (20) is the same as the ratio  $F_e/G_e$  for  $\lambda = 1/1000$  ( $1/20$ ). We find

$$\frac{F_e}{G_e} = \frac{1}{2} \left( 1 - \frac{m_e}{m_p + m_e} \frac{v_r^2}{2} \right) \quad (6.1)$$

for low velocities.

In Fig. 6 we show graphs of  $F_p/F_e$  vs  $v_r^2$  for stable solutions for mass ratios  $\lambda = 1, 20, 1000$ . In the equal-mass case and in the nonrelativistic limit  $F_p/F_e$  equals unity as expected, but for  $\lambda > 1$  and  $0 < v_r^2 < 1$ ,  $F_p/F_e$  is less than unity, meaning that the radial amplitude of perturbation divided by the radius of the circular orbit is less for the heavy particle than for the light one. For low velocities we find

$$\frac{F_p}{F_e} = 1 - \frac{m_p - m_e}{m_p + m_e} \frac{v_r^2}{2} \quad (6.2)$$

which, with Eq. (6.1), yields  $G_p = G_e$ . For reasons unknown to us the dashed ( $D^{(-)}$ ) curves of Figs. 4 and 5 are nearly alike.

## VII. CONCLUSIONS

We have shown for certain high-velocity circular orbits in the two-body problem that there exist (in first-order perturbation theory) several stable

perturbations which all have the same average angular velocity. We interpret this to mean that, in such cases at least, Newtonian initial conditions do not determine the subsequent motion. The system has more than the usual number of degrees of freedom. Such an effect has been the subject of many speculations but has not previously been demonstrated using the exact equations of time-symmetric action-at-a-distance electrodynamics. In particular, this effect has been used by Plass to derive the Rayleigh-Jeans blackbody radiation law.

In addition we have found an infinite number of divergent perturbations for any given circular orbit, regardless of how low the velocity may be. Since the divergent perturbations involve trajectories with large deviations from the circular orbits, first-order perturbation theory is not powerful

enough to study them. There may or may not exist full mathematical solutions which have small sections of their trajectories which are almost like small sections of trajectories of the bound circular orbits.

The question as to the necessity of a selection principle for ruling out certain solutions remains open.

#### VIII. ACKNOWLEDGMENTS

We would like to thank the Aspen Center for Physics for its hospitality during the summer of 1971 when part of this work was done. In addition one of us (C.M.A.) would like to acknowledge conversations with R. N. Hill, W. R. Melvin, and G. T. Rublein.

#### APPENDIX

The radial equation of motion for particle  $e$  is

$$0 = A_{e02}\ddot{\rho}_e(t) + \frac{1}{2}A_{p+2}[\ddot{\rho}_p(t-\tau) + \ddot{\rho}_p(t+\tau)] + \frac{1}{2}A_{p-2}[\ddot{\epsilon}_p(t-\tau) - \ddot{\epsilon}_p(t+\tau)] + A_{e01}\dot{\epsilon}_e(t) + \frac{1}{2}A_{p+1}[\dot{\epsilon}_p(t-\tau) + \dot{\epsilon}_p(t+\tau)] + \frac{1}{2}A_{p-1}[\dot{\rho}_p(t-\tau) - \dot{\rho}_p(t+\tau)] + A_{e00}\rho_e(t) + \frac{1}{2}A_{p+0}[\rho_p(t-\tau) + \rho_p(t+\tau)] + \frac{1}{2}A_{p-0}[\epsilon_p(t-\tau) - \epsilon_p(t+\tau)], \quad (A1)$$

where

$$\begin{aligned} A_{e02} &= 1, \\ A_{p+2} &= -v_p V_e^{-1}(v_e \theta_0 + v_p \sin \theta_0)(v_p \theta_0 + v_e \sin \theta_0), \\ A_{p-2} &= v_p V_e^{-1}(v_e \theta_0 + v_p \sin \theta_0)(v_p + v_e \cos \theta_0), \\ A_{e01} &= \omega_0 \{-2 - v_e^2/(1 - v_e^2) + v_e v_p V_e^{-1}[v_p + v_e \cos \theta_0 + v_e \theta_0 \sin \theta_0 + v_e v_p(v_e + v_p \cos \theta_0)]\}, \\ A_{p+1} &= \omega_0 v_p \{-3 v_e \sin \theta_0 / (\theta_0 + v_e v_p \sin \theta_0) + V_e^{-1}[\sin \theta_0 (\theta_0 + v_e v_p \sin \theta_0) - 2 \theta_0^2 \cos \theta_0 \\ &\quad + 2 v_e^2 \theta_0 \sin \theta_0 + 3 v_e (v_e + v_p \cos \theta_0)(\cos \theta_0 + v_e v_p)]\}, \\ A_{p-1} &= \omega_0 v_p \{-3 (v_p + v_e \cos \theta_0) / (\theta_0 + v_e v_p \sin \theta_0) + V_e^{-1}[\theta_0 \cos \theta_0 (1 + 2 v_e^2 - v_p^2) \\ &\quad + 2 v_e v_p \theta_0 + \sin \theta_0 (2 v_p^2 - v_e^2 + 2 v_e v_p \cos \theta_0) + v_e^2 v_p^2 \sin \theta_0]\}, \\ A_{e00} &= \omega_0^2 \{-1 - v_e^2 / (1 - v_e^2) - 3 v_e v_p \sin \theta_0 / (\theta_0 + v_e v_p \sin \theta_0) \\ &\quad + v_e V_e^{-1}[1 + v_p^2 (1 + \cos^2 \theta_0) + 2 v_e v_p (\theta_0 \sin \theta_0 + 2 \cos \theta_0) + 3 v_e^2 v_p^2 + 2 v_e v_p^3 \cos \theta_0] + v_e (v_e + v_p \cos \theta_0) \Gamma\}, \\ A_{p+0} &= \omega_0^2 v_p \{-3 v_e \sin \theta_0 / (\theta_0 + v_e v_p \sin \theta_0) + V_e^{-1}[\cos \theta_0 (1 + v_e^2 - v_p^2 + 3 v_e^2 v_p^2) \\ &\quad + (1 + v_e^2)(2 v_e v_p + \theta_0 \sin \theta_0)] + (v_p + v_e \cos \theta_0) \Gamma\}, \\ A_{p-0} &= \omega_0^2 v_p \{3 v_e \cos \theta_0 / (\theta_0 + v_e v_p \sin \theta_0) - V_e^{-1}[\theta_0 \cos \theta_0 - (1 - \theta_0^2) \sin \theta_0 \\ &\quad - v_e v_p \sin \theta_0 (v_e v_p + 2 \cos \theta_0) + v_e^2 (\theta_0 \cos \theta_0 - 2 \sin \theta_0)] + v_e \sin \theta_0 \Gamma\}, \end{aligned} \quad (A2)$$

$$V_e = v_e + v_p (\cos \theta_0 - \theta_0^2 \cos \theta_0 + \theta_0 \sin \theta_0) + v_e^2 v_p (2 \cos \theta_0 + \theta_0 \sin \theta_0) + v_e v_p^2 (1 + \cos^2 \theta_0) + v_e^2 v_p^2 (v_e + v_p \cos \theta_0),$$

$$\Gamma = [-3(1 + v_e v_p \cos \theta_0) / (\theta_0 + v_e v_p \sin \theta_0) + v_p V_e^{-1}(1 - v_e^2)(v_p^2 \sin \theta_0 - \theta_0 \cos \theta_0)] / (\theta_0 + v_e v_p \sin \theta_0).$$

The tangential equation of motion for particle  $e$  is

$$0 = B_{e02}\ddot{\epsilon}_e(t) + \frac{1}{2}B_{p+2}[\dot{\epsilon}_p(t-\tau) + \dot{\epsilon}_p(t+\tau)] + \frac{1}{2}B_{p-2}[\dot{\rho}_p(t-\tau) - \dot{\rho}_p(t+\tau)] + B_{e01}\dot{\rho}_e(t) + \frac{1}{2}B_{p+1}[\dot{\rho}_p(t-\tau) + \dot{\rho}_p(t+\tau)] + \frac{1}{2}B_{p-1}[\dot{\epsilon}_p(t-\tau) - \dot{\epsilon}_p(t+\tau)] + B_{e00}\epsilon_e(t) + \frac{1}{2}B_{p+0}[\epsilon_p(t-\tau) + \epsilon_p(t+\tau)] + \frac{1}{2}B_{p-0}[\rho_p(t-\tau) - \rho_p(t+\tau)], \quad (A3)$$

where

$$\begin{aligned}
B_{e02} &= 1, \\
B_{p+2} &= v_p V_e^{-1} (1 - v_e^2) (v_e + v_p \cos \theta_0) (v_p + v_e \cos \theta_0), \\
B_{p-2} &= -v_p V_e^{-1} (1 - v_e^2) (v_e + v_p \cos \theta_0) (v_p \theta_0 + v_e \sin \theta_0), \\
B_{e01} &= \omega_0 [2 - v_e V_e^{-1} (\theta_0 + v_e v_p \sin \theta_0)^2], \\
B_{p+1} &= \omega_0 v_p V_e^{-1} (1 - v_e^2) [-3 v_p (v_p + v_e \cos \theta_0) \mathfrak{W} - (1 - v_p^2) \theta_0 \sin \theta_0 + 2 (v_e + v_p \cos \theta_0) (v_p + v_e \cos \theta_0)], \\
B_{p-1} &= \omega_0 v_p V_e^{-1} (1 - v_e^2) [-3 v_e v_p \sin \theta_0 \mathfrak{W} + \theta_0 \cos \theta_0 + 2 \theta_0^2 \sin \theta_0 + 3 v_e v_p \theta_0 - 2 v_e v_p \sin \theta_0 \cos \theta_0], \\
B_{e00} &= \omega_0^2 \{-1 + v_e V_e^{-1} [-3 (1 - v_e^2) v_p^2 \cos \theta_0 \mathfrak{W} + 1 + 2 v_p^2 - v_p^2 \cos^2 \theta_0 \\
&\quad + 2 v_e v_p \theta_0 \sin \theta_0 + 3 v_e v_p \cos \theta_0 - v_e^3 v_p \cos \theta_0] - v_e v_p \sin \theta_0 \Delta\}, \\
B_{p+0} &= \omega_0^2 v_p V_e^{-1} (1 - v_e^2) [3 v_e v_p \cos \theta_0 \mathfrak{W} + \cos \theta_0 - \theta_0^2 \cos \theta_0 + \theta_0 \sin \theta_0 - v_e v_p (1 - 2 \cos^2 \theta_0)] + \omega_0^2 v_e v_p \sin \theta_0 \Delta, \\
B_{p-0} &= \omega_0^2 v_p V_e^{-1} (1 - v_e^2) [-3 v_e v_p \sin \theta_0 \mathfrak{W} + \theta_0 \cos \theta_0 - \sin \theta_0 + \theta_0^2 \sin \theta_0 + 2 v_e v_p (\theta_0 - \sin \theta_0 \cos \theta_0)] - \omega_0^2 v_p (v_p + v_e \cos \theta_0) \Delta, \\
\mathfrak{W} &= [\theta_0 \cos \theta_0 - (1 - \theta_0^2) \sin \theta_0 + v_e v_p (\theta_0 - \sin \theta_0 \cos \theta_0)] / (\theta_0 + v_e v_p \sin \theta_0), \\
\Delta &= v_p V_e^{-1} (1 - v_e^2) [3 (1 + v_e v_p \cos \theta_0) \mathfrak{W} - \theta_0^2 \cos \theta_0 - \theta_0 \sin \theta_0 - 2 v_e v_p \sin^2 \theta_0] / (\theta_0 + v_e v_p \sin \theta_0).
\end{aligned} \tag{A4}$$

Some general relations which hold among these quantities are

$$\begin{aligned}
A_{e+2} B_{e+2} &= A_{e-2} B_{e-2}, \\
A_{p+2} B_{p+2} &= A_{p-2} B_{p-2}, \\
B_{e00} &= -B_{p+0}, \\
B_{p00} &= -B_{e+0}.
\end{aligned} \tag{A5}$$

- <sup>1</sup>J. A. Wheeler and R. P. Feynman, *Rev. Mod. Phys.* **17**, 157 (1945); **21**, 425 (1949).  
<sup>2</sup>A. Schild, *Phys. Rev.* **131**, 2762 (1963).  
<sup>3</sup>Circular orbits are solutions of a wide range of theories. Cf. C. M. Andersen and H. C. von Baeyer, *Ann. Phys. (N.Y.)* **60**, 67 (1970).  
<sup>4</sup>C. G. Darwin, *Phil. Mag.* **39**, 537 (1920).  
<sup>5</sup>J. L. Anderson, *Principles of Relativity Physics* (Academic, New York, 1967), p. 225.  
<sup>6</sup>E. Breitenberger, *Am. J. Phys.* **36**, 505 (1968).  
<sup>7</sup>J. L. Synge, *Proc. Roy. Soc. (London)* **A177**, 118 (1940).  
<sup>8</sup>A. Sommerfeld, *Ann. Physik* **51**, 1 (1915); J. L. Synge, *Relativity: The Special Theory* (Interscience, New York, 1956), p. 396.  
<sup>9</sup>E. H. Kerner, *J. Math. Phys.* **3**, 35 (1962); **6**, 1218 (1965).  
<sup>10</sup>F. J. Kennedy, *J. Math. Phys.* **10**, 1349 (1969).  
<sup>11</sup>R. D. Driver, *Phys. Rev.* **178**, 2051 (1969).  
<sup>12</sup>G. N. Plass, Ph.D. thesis, Princeton, 1947 (unpublished). We are indebted to Professor J. A. Wheeler for

pointing out this work to us.

- <sup>13</sup>For a different approach, cf. D. Leiter, *Am. J. Phys.* **38**, 207 (1970).  
<sup>14</sup>R. E. Bellman and K. L. Cooke, *Differential-Difference Equations* (Academic, New York, 1963).  
<sup>15</sup>A. Staruszkiewicz, *Acta Phys. Polon.* **33**, 1007 (1968).  
<sup>16</sup>A. Staruszkiewicz, *Ann. Physik* **23**, 66 (1969).  
<sup>17</sup>F. Rohrlich, *Classical Charged Particles* (Addison-Wesley, Reading, Mass., 1965), p. 134.  
<sup>18</sup>H. Van Dam and E. P. Wigner, *Phys. Rev.* **138**, B1576 (1965); **142**, 838 (1966).  
<sup>19</sup>Introductory note, by J. A. Wheeler, to the 1945 paper of Ref. 1.  
<sup>20</sup>Professor R. N. Hill has pointed out to us that this discrepancy is removed if one includes terms in  $e^4$  as well.  
<sup>21</sup>These are discussed at length in Chap. 12 of Ref. 14. We follow this source.  
<sup>22</sup>Equation (15) of Ref. 15 corresponds to our Eq. (4.9).